Distribution and production of reactive mercury and dissolved gaseous mercury in surface waters and water/air mercury flux in reservoirs on Wujiang River, Southwest China

Xuewu Fu, Xinbin Feng, Yanna Guo, Bo Meng, Runsheng Yin, Heng Yao

Distribution and production of reactive mercury and dissolved gaseous mercury in surface waters and water/air mercury flux in reservoirs on Wujiang River, Southwest China

Xuewu Fu,[1,2] Xinbin Feng,[1] Yanna Guo,[3] Bo Meng,[1] Runsheng Yin,[1] and Heng Yao[1]

Received 20 December 2012; revised 1 April 2013; accepted 3 April 2013; published 13 May 2013.

[1] Transformation and distribution of mercury (Hg) species play an important role in the biogeochemical cycling of mercury in aquatic systems. Measurements of water/air exchange fluxes of Hg, reactive mercury (RHg), and dissolved gaseous mercury (DGM) concentrations were conducted at 14 sites in five reservoirs on the Wujiang River, Guizhou, Southwest China. Clear spatial and temporal variations in Hg fluxes, RHg, and DGM concentrations were observed in the study area. Hg fluxes and RHg concentrations exhibited a consistent diurnal variation in the study area, with maximum fluxes and concentrations during daytime. A typical diurnal trend of DGM with elevated concentration at night was observed in a eutrophic reservoir with elevated bacteria abundance, suggesting a bacteria-induced production of DGM in this reservoir. For other reservoirs, a combination of sunlight-stimulated production and loss via photo-induced oxidation and evaporation regulated the diurnal trends of DGM. Seasonal variations with elevated Hg fluxes and RHg concentrations in warm season were noticeable in the study area, which highlighted the combined effect of interrelationships between Hg species in water and environmental parameters. Hg fluxes exhibited much more significant correlations with RHg and THg concentrations and air temperature compared to DGM concentrations and solar radiation. The measured fluxes were significantly higher than those simulated using the water/air thin film Hg^0 gradient model. Aside from the potential limitations of dynamic flux chamber method, this may also suggest the thin film gas exchange model is not capable of predicting water/air Hg flux under low wind speed conditions. Additionally, it is speculated that DGM concentrations might vary significantly in surface waters with depth, and measurements of DGM at a depth of 2–4 cm below the water surface probably underestimated the DGM concentration that should be taken into account in simulations of water/air flux using the thin film gas exchange model. An empirical model of water/air Hg flux was developed, and the simulated fluxes were compared well with measurements. The model yields a mean annual Hg emission of 3.2 ± 1.0 kg in the study area.

Citation: Fu, X., X. Feng, Y. Guo, B. Meng, R. Yin, and H. Yao (2013), Distribution and production of reactive mercury and dissolved gaseous mercury in surface waters and water/air mercury flux in reservoirs on Wujiang River, Southwest China, *J. Geophys. Res. Atmos.*, *118*, 3905–3917, doi:10.1002/jgrd.50384.

1. Introduction

[2] Studying speciation and transformation of mercury (Hg) is a crucial step in understanding Hg fate in the aquatic environments. Reactive Hg (RHg) and dissolved gaseous Hg (DGM) are the two important inorganic fractions of total mercury (THg) in aquatic environments. DGM is composed primarily of elemental mercury (Hg^0) in freshwaters, and RHg (includes DGM and "easily reducible" Hg species) is operationally defined as a fraction of THg that is easily reducible with the addition of $SnCl_2$ [*Rolfhus and Fitzgerald*, 2001]. Although RHg and DGM constitute a small portion of THg in aquatic systems [*Krabbenhoft et al*., 1998; *Garcia et al*., 2006; *Zhang et al*., 2006a], it is of a great importance to study the fate of RHg and DGM due to their connections to both Hg methylation in aquatic systems and Hg emission from water environments [*Xu et al*., 1999; *Gårdfeldt et al*., 2003a; *Marvin-DiPasquale and Cox*, 2007; *Skyllberg et al*., 2009].

[1]State Key Laboratory of Environmental Geochemistry, Institute of Geochemistry, Chinese Academy of Sciences, Guiyang, China.
[2]Observatoire Midi-Pyrénées, Géosciences Environnement Toulouse, CNRS/IRD/Université Paul Sabatier Toulouse 3, Toulouse, France.
[3]HydroChina Guiyang Engineering Corporation, Guiyang, China.

Corresponding author: X. Feng, State Key Laboratory of Environmental Geochemistry, Institute of Geochemistry, Chinese Academy of Sciences, Guiyang 550002, China. (fengxinbin@vip.skleg.cn)

2169-897X/13/10.1002/jgrd.50384

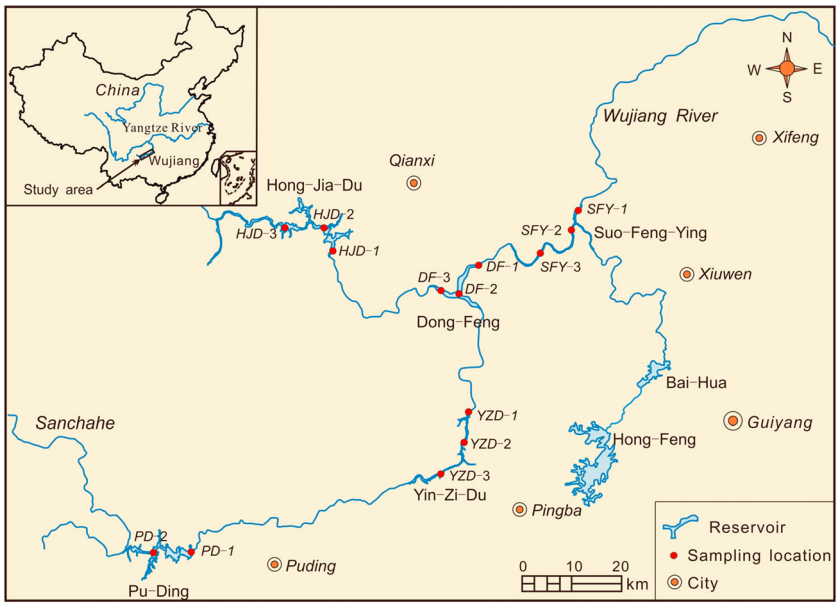

Figure 1. Study area and sampling locations.

[3] The production of DGM in water is known to be stimulated by abiotic and biotic processes. Sunlight-induced reduction is an important mechanism in contributing to DGM production in surface waters, as evidenced by many well-characterized diurnal cycles with increasing DGM concentrations during daytime in both freshwaters and seawaters which are strongly related to the intensity of solar radiation [*O'Driscoll et al*., 2008; *Zhang et al*., 2006a; *Qureshi et al*., 2010]. The sunlight-induced production of DGM is also proposed to be facilitated by ferric iron (Fe(II)), phytoplankton photosynthetic activities, and dissolved organic carbon [*Xiao et al*., 1995; *Zhang and Lindberg*, 2001; *Poulain et al*., 2004; *Peters et al*., 2007]. Microbial activity has also been suggested to contribute to DGM production in waters, and it may better explain the net accumulation of DGM at deeper layers of lakes [*Amyot et al*., 1997; *O'Driscoll et al*., 2008]. Additionally, a study in Mystic Lake suggested that microbial activities (primary heterotrophic bacteria) were responsible for DGM production in the upper water layers, and this process was still activated in the absence of sunlight [*Mason et al*., 1995].

[4] The information on the production and distribution of RHg in aquatic environments is relatively limited. Some studies in laboratory demonstrated that DGM in waters could be oxidized in both dark and sunlight conditions [*Lalonde et al*., 2004; *Amyot et al*., 2005], which could be a possible source for RHg occurring in water environments. In most cases, however, RHg concentrations in water were much higher than DGM concentrations [*Krabbenhoft et al*., 1998; *Rolfhus and Fitzgerald*, 2001; *Zhang et al*., 2006a], and this suggests oxidation of DGM is not the major mechanism in contributing to RHg in waters. It was also proposed that sunlight-stimulated desorption of Hg(II) from suspended solid substrate plays an important role in RHg production in waters [*Krabbenhoft et al*., 1998].

[5] Water and air exchange flux of Hg is mainly driven by the production of Hg^0 in the surface water. Strong correlations between Hg flux and weather parameters have been well established in previous studies [*Poissant and Casimir*, 1998; *Boudala et al*., 2000; *Feng et al*., 2004, 2008]. Additionally, enhanced emission fluxes of Hg as a function of elevated dissolved organic carbon (DOC) content were also observed by previous studies [*Costa and Liss*, 2000; *Gårdfeldt et al*., 2001; *Fu et al*., 2010a]. On the other hand, however, the interrelationships underlying THg, RHg, and DGM concentrations and Hg flux have not been well characterized in freshwater environments. Also, many of the previous studies were conducted at one sampling site and in a relatively short sampling period, and therefore, it is not clear whether the environmental factors related to the diurnal variations still dominate the spatial and seasonal variations of mercury forms and fluxes in different waters. In the present study, measurements of THg, RHg, and DGM in surface waters and Hg fluxes were monitored at 14 sites in five reservoirs in Wujiang River basin, Southwest China. Both seasonal and diurnal variations of RHg, DGM, and Hg fluxes were also investigated. The objectives of this study were the following: (1) to examine the diurnal and seasonal trends of RHg, DGM, and Hg flux in fresh water systems; (2) to evaluate the major variables controlling the temporal and spatial variations of RHg, DGM, and Hg fluxes; (3) to establish overall correlations between Hg fluxes and weather parameters, THg, RHg, and DGM concentrations; and (4) to develop an empirical model for predicting Hg fluxes from freshwater surface. This work is supposed to be useful in better understanding Hg dynamics in water systems and assessing water emissions of Hg to the local, regional, and global atmosphere.

2. Experimental Method

2.1. Study Area and Sampling Locations

[6] The field experiments were carried out in five reservoirs on the upper branches of Wujiang River, which is one of the biggest branches of the upper Yangtze River (Figure 1). Some relevant information about the studied reservoirs including

Table 1. Basic Parameters of the Studied Reservoirs

	HJD (Hongjiadu) Reservoir	PD (Puding) Reservoir	YZD (Yinzidu) Reservoir	DF (Dongfeng) Reservoir	SFY (Suofengying) Reservoir
Operation time	2004	1993	2003	1994	2005
Immersed area (m^2)	80.5×10^6	19.2×10^6	15.0×10^6	19.1×10^6	5.7×10^6
Storage capacity (m^3)	33.6×10^8	2.5×10^8	3.2×10^8	4.9×10^8	0.7×10^8
Max depth (m)	110	45	100	110	90
Water residence time (day)	380	27	37	33	7
Altitude (m above sea level)	1130	1145	1088	970	837
Water flow rate ($cm\,s^{-1}$)	0.04	0.4	0.4	1.0	5.2
Precipitation depth (mm)	881	1203	1068	970	976
Mean solar radiation ($w\,m^{-2}$)	112	111	97	98	98
Mean air temperature (°C)	12.8	14.1	14.5	14.0	14.1
Wet Hg deposition flux ($\mu g\,m^{-2}\,h^{-1}$) [*Guo et al*., 2008a]	34.7	24.8	38.1	36.3	-

immersed area, normal storage capacity, maximum depth, altitude, and meteorological parameters during the sampling campaigns are shown in Table 1. For each reservoir, two to three sampling sites were selected to describe the spatial distributions of RHg, DGM, and Hg flux, which were located near the dam, at the middle, and at the upper reach of the reservoirs, respectively (Figure 1). Measurements of water/air exchange flux of Hg were conducted at each of the sampling sites in both the warm season (July to October) and cold season (November, December, and January). Measurements of RHg and DGM concentrations in surface water at HJD and PD reservoirs were carried out in warm and cold seasons, and those at DF and YZD reservoirs were performed in cold season. The measurements of Hg flux at each site were conducted continuously for more than 24 h to present a full diurnal pattern, and RHg and DGM concentrations were measured continuously from early morning to midnight at an interval of 1 h. A sample for THg concentration analysis at each of the sampling sites was also collected from surface water during the sampling campaign of Hg flux, RHg, and DGM measurements.

2.2. Measurements of Water/Air Exchange Flux of Hg

[7] Exchange flux of Hg between water and atmosphere was monitored by using a dynamic flux chamber (DFC) method [*Poissant and Casimir*, 1998; *Gårdfeldt et al*., 2001; *Feng et al*., 2008]. A semicylinder, open-bottom quartz glass chamber ($Ø20 \times 60$ cm, $V = 0.009\,m^3$) was placed on a bottom-open floating boat at the water/air interface. Water/air Hg flux was obtained via measuring the difference in atmospheric Hg concentrations inside and outside the flux chamber and exchange flux of air mass in the chamber. Water/air exchange flux of Hg was estimated using equation (1):

$$F = (C_o\text{-}C_i) \times Q/A \quad (1)$$

where F is the Hg flux in $ng\,m^{-2}\,h^{-1}$; C_o and C_i are the Hg concentrations of the outlet and inlet air stream ($ng\,m^{-3}$), respectively; A is the enclosed water area ($0.12\,m^2$); and Q is the flushing flow rate through the chamber (8–15 L min^{-1}). Hg concentrations of the inlet and outlet air were measured using an automated Hg vapor analyzer (Tekran 2537A). Alternate measurements of air Hg concentrations from the inlet to the outlet of the chamber every 10 min were achieved by using a magnetic three-way valve (Tekran 1110). The data quality of Tekran Model 2537A was guaranteed via periodic internal calibration at a 25 h interval. It was suggested that flushing flow rate and associated chamber turnover time (TOT) have a crucial influence on Hg flux from soil (*Eckley et al*., 2010). To the best of our knowledge, studies on the role of flushing flow rate in Hg flux from waters are very limited. The study on soil/air exchange flux of Hg by *Eckley et al*. [2010] suggested that a TOT of 0.84 min could be adopted for substrates with low Hg concentrations. The chamber TOTs in the present study were in the range of 0.7–1.2 min, which are consistent with that proposed for low Hg substrates by *Eckley et al*. [2010]. Blanks of the chamber were measured with an ultra clean quartz glass plate and in the range of -0.12–$0.28\,ng\,m^{-2}\,h^{-1}$ ($mean = 0.07 \pm 0.18\,ng\,m^{-2}\,h^{-1}$). The detection limit (based on 3 times the standard deviation of blanks) of the DFC system was estimated to be $0.5\,ng\,m^{-2}\,h^{-1}$. The blanks were small, and we did not make blank correction for measured fluxes.

2.3. Analysis of RHg, DGM, and THg Concentrations in Surface Water

[8] RHg and DGM concentrations in surface waters were determined on an experimental boat within 1–2 min after the collection of water samples, and this was supposed to minimize risks of contamination and/or loss of RHg and DGM. THg concentrations in surface waters were analyzed in the laboratory. Water samples were collected about 10 m away from the reservoir bank and at a depth of 2–4 cm below the water surface. A volume of 1 L water was collected for analysis of RHg and DGM using two 1.5 L precleaned borosilicate glass bottles. Before filling with 1 L of samples, sampling bottles were cleaned three times with the surface water in the reservoir. For RHg analysis, 1.5 mL $SnCl_2$ solution was firstly added to the water samples, and then the reduced Hg^0 was collected on a gold trap by purging the samples with Hg-free argon gas for 30 min at 300–400 mL min^{-1}. DGM in water samples was directly extracted onto a gold trap by purging the sample in the manner similar as RHg. The purging time is an important parameter for complete extraction of DGM and RHg from waters and depending on water volume, purging flow rate, and water temperature [*Gårdfeldt et al*., 2002]. Given the sample volume of 1 L and purging flow rate of 300–400 mL min^{-1} in the present study, extraction efficiencies of ~97% and 90% were expected in warm (20–25°C) and cold seasons (10–15°C), respectively. The borosilicate glass bottles

were wrapped with foil sheet during bubbling to block out sunlight. To avoid water condensation and passivation of gold trap, soda lime traps were implemented, and the gold traps were also kept at a temperature of approximately 50°C. RHg and DGM collected on gold traps were determined by dual amalgamation combined with cold vapor atomic fluorescence spectroscopy (CVAFS) detection. THg concentrations in surface waters were determined in the laboratory using the standard method of BrCl oxidation followed by $SnCl_2$ reduction, purge and trap, and dual amalgamation combined with CVAFS detection [*Feng et al*., 2009a, 2009b].

[9] The borosilicate glass bottles and impingers used in this study were acid-cleaned followed by baking in a Muffle furnace at 500°C for 1.0 h. $SnCl_2$ solution was purged overnight with Hg-free argon at 400 mL min^{-1} to remove all traces of Hg. To ensure clean operation, polyethylene gloves were used throughout the field operations. Blank checks were preformed before field sampling and analysis. The average blanks for DGM ($n = 8$), RHg ($n = 13$), and THg ($n = 12$) were 1.6 ± 0.6 pg L^{-1}, 8.7 ± 3.1 pg L^{-1}, and 0.02 ± 0.01 ng L^{-1}, respectively. The detection limits for DGM, RHg, and THg were 1.8 pg L^{-1}, 9.0 pg L^{-1}, and 0.03 ng L^{-1}, respectively, which were obtained by 3 times the standard deviation of blanks.

2.4. Meteorological and Water Quality Parameters

[10] Meteorological parameters were continuously monitored at the sampling sites using a portable weather station (Puhui, Wuhan, China). Air temperature (accuracy ±0.1°C), air relative humidity (accuracy ± 1%), solar radiation (accuracy ± 5%), wind speed (accuracy ±0.3 m s^{-1}), and wind direction (accuracy ± 1%) were measured at 2 m height above the water surface on the reservoir bank. Water temperature was measured near the sampling site using a temperature probe (Puhui, Wuhan, China, accuracy ± 0.1°C). DOC content in water was measured using a high-temperature combustion method [*Cosovic et al*., 2000]. Total suspended solids (TSS) concentration was measured by collecting and weighing suspended particles from a measured volume of water sample (1.5 L) with Teflon filter (Minipore, 0.45 μm). pH value of water was measured using a portable analyzer (PD-501, Shanghai, China). Turbidity and clarity of water (Secchi depth) at the sampling site was measured each hour from 9 A.M. to 3 P.M. using a modified Secchi disk.

2.5. Modeled Hg Fluxes and Saturation of DGM

[11] Modeled water/air flux of Hg was calculated using a thin film gas exchange model developed by *Wanninkhof* [1992]. The degree of DGM supersaturation, SS, was calculated using equations (2) and (3):

$$SS = DGM \times H'(T)/GEM - 1 \quad (2)$$

$$H'(T) = \exp(-2404.3/T + 6.92) \quad (3)$$

where DGM is the concentration of Hg^0 in water (pg L^{-1}), GEM is the concentration of Hg^0 in ambient air above water surface (ng m^{-3}), H′(T) is the dimensionless partitioning coefficient for Hg^0 between freshwater and air as known as the Henry's law constant [*Andersson et al*., 2008], and T is the water temperature in K.

[12] The water/air exchange flux of Hg, F (ng m^{-2} h^{-1}), was calculated using equation (4):

$$F = K_w \times (DGM - GEM/H'(T)) \quad (4)$$

where K_w is the gas transfer velocity of a Hg^0 in the water/air surface (cm h^{-1}) and was calculated according to equation (5) [*Wanninkhof*, 1992]:

$$Kw = 0.31 \times {U_{10}}^2 \times \left(Sc_{Hg}/600\right)^{-0.5} \quad (5)$$

where U_{10} is the wind speed normalized to 10 m above water surface, and Sc_{Hg}, the Schmidt number for Hg, is defined as follows:

$$Sc_{Hg} = \nu/D_{Hg} \quad (6)$$

where ν is the kinematic viscosity (cm^2 s^{-1}) of freshwater, and DHg is the Hg diffusion coefficient (cm^2 s^{-1}) in freshwater, which was calculated by the molecular dynamics simulation, as described by *Kuss et al*. [2009].

3. Results and Discussion

3.1. Spatial and Temporal Distributions of Water Mercury Species and Mercury Flux

[13] Mean RHg concentrations in DF, YZD, PD, and HJD reservoirs in the study area varied from 42.2 to 184.9 pg L^{-1}, and the ratio of RHg to THg in the study area were in the range of 2.9–10.8%. Average DGM concentrations at the study sites ranged from 7.8 to 40.0 pg L^{-1}, accounting for approximately 14.7–36.1% and 0.5–2.8% of the RHg and THg in surface waters, respectively. The levels of RHg and DGM in the study area were consistent with the results measured in the surface water of Florida Everglades, USA [*Krabbenhoft et al*., 1998] but much lower than those observed in the Hongfeng reservoir, Southwest China [*Feng et al*., 2008] and Bay Saint François wetlands, Canada [*Zhang et al*., 2006a].

[14] Evasion of Hg from water surface to the atmosphere was the predominant process throughout the whole sampling campaigns, with the 24 h mean Hg fluxes in the range of 0–4.3 ng m^{-2} h^{-1}. Water/air Hg fluxes in the study area were relatively lower than those measured in the Hongfeng and Baihua Reservoirs (1.8–7.4 ng m^{-2} h^{-1}), which were impacted by significant discharges of municipal sewage from urban areas [*Feng et al*., 2004, 2008]. Hg fluxes presented in this study were also lower than the fluxes observed in Wujiangdu reservoir (3.2–20.1 ng m^{-2} h^{-1}), which was a hypereutrophic reservoir with increasing microbial activities [*Fu et al*., 2010a].

[15] RHg and DGM concentrations exhibited a clear spatial variation in the study area. RHg and DGM concentrations in cold season were comparable among PD, SFY, and DF reservoirs (t test, $p_{RHg} < 0.37$, $p_{DGM} < 0.14$), but they were approximately 2 times lower than the concentrations observed in HJD reservoir. In warm season, RHg and DGM concentrations in HJD reservoir were also relatively higher than those observed in PD reservoir (Table 2, measurements of RHg and DGM in warm season were only carried out in HJD and PD reservoirs). Some of the weather and water chemistry

Table 2. Statistical Summary of Hg Fluxes (24 h Means), Total Gaseous Mercury (TGM), RHg, DGM Concentrations, DGM Supersaturation (DGM SS), and Environmental Parameters at Sites in the Study Area

Site	Season	Hg Flux ($ng\,m^{-2}\,h^{-1}$)	TGM Concentration ($ng\,m^{-3}$)	THg Concentration ($ng\,L^{-1}$)	RHg Concentration ($pg\,L^{-1}$)	DGM Concentration ($pg\,L^{-1}$)	Solar Intensity ($w\,m^{-2}$)	Air Temperature (°C)	Water Temperature (°C)	DGM SS	Modeled Hg Flux ($ng\,m^{-2}\,h^{-1}$)	Light Transmittance (m)	Wind Speed ($m\,s^{-1}$)	TSS ($mg\,L^{-1}$)
HJD-1	Warm	4.2 ± 3.9	3.8 ± 1.8	1.91	184.9 ± 30.2	40.0 ± 20.6	209 ± 303	27.1 ± 3.1	24.1 ± 0.4	1.8 ± 1.2	0.2 ± 0.3	2.6 ± 0.2	1.3	0.71
HJD-3	Warm	4.2 ± 3.1	2.6 ± 1.5	1.53	165.9 ± 31.0	24.4 ± 6.3	251 ± 339	27.2 ± 2.8	24.4 ± 0.4	2.6 ± 2.6	0.2 ± 0.2	3.1 ± 0.2	1.3	0.53
HJD-1	Cold	3.1 ± 4.1	6.4 ± 1.0	1.66			124 ± 212	12.8 ± 3.2	16.5 ± 0.2			5.9 ± 0.5	0.6	0.07
HJD-2	Cold	2.7 ± 3.8	6.7 ± 2.4	1.84	121.1 ± 30.3	39.0 ± 4.5	76 ± 167	13.4 ± 3.0	16.6 ± 0.1	0.4 ± 0.5	0.1 ± 0.1	6.9 ± 0.2	0.9	0.08
HJD-3	Cold	2.1 ± 2.6	7.8 ± 2.8	1.35	111.4 ± 18.4	37.9 ± 10.3	115 ± 205	11.9 ± 2.8	16.4 ± 0.0	0.4 ± 0.3	0 ± 0.2	6.3 ± 0.4	0.3	0.07
PD-1	Warm	2.2 ± 1.2	2.4 ± 1.5	1.77	95.1 ± 9.7	21.9 ± 5.0	49 ± 11587	21.7 ± 1.0	23.2 ± 0.1	3.1 ± 3.2	0 ± 0	2.6 ± 0.2	0.1	
PD-2	Warm	4.2 ± 5.3	2.8 ± 0.8	2.14	109.2 ± 23.6	26.4 ± 15.6	107 ± 157	24.3 ± 2.3	24.0 ± 0.3	2.0 ± 1.3	0.8 ± 0.8	2.2 ± 0.2	2.3	
PD-1	Cold	0 ± 1.0	4.9 ± 1.4	1.06	49.2 ± 5.6	14.6 ± 2.3	104 ± 160	14.8 ± 1.5	12.5 ± 0.1	−0.3 ± 0.2	−0.1 ± 0.2	3.2 ± 0.2	1.2	1.5 ± 0.5
PD-2	Cold	0.2 ± 0.9	5.3 ± 0.7	1.27	57.1 ± 3.0	20.6 ± 2.1	7 ± 14	7.2 ± 2.6	12.1 ± 0.1	−0.1 ± 0.2	0 ± 0.1	3.0 ± 0.2	1.4	2.0 ± 0.5
YZD-1	Warm	4.0 ± 6.1	3.7 ± 1.5	2.86			163 ± 256	23.7 ± 2.9						1.4
YZD-2	Warm	3.9 ± 4.7	3.6 ± 1.1	2.94			116 ± 189	22.4 ± 1.7						1.5
YZD-3	Warm	4.0 ± 2.5	5.0 ± 1.2	3.18			22 ± 41	16.9 ± 1.5						1.7
YZD-1	Cold	0.1 ± 0.9	14.1 ± 4.0	0.65	67.0 ± 17.1	17.8 ± 2.2	9 ± 15	9.0 ± 1.2	14.5 ± 0.0	−0.6 ± 0.1	−0.1 ± 0	4.3 ± 0.1	0.7	0.5
YZD-2	Cold	0.4 ± 0.7	9.7 ± 1.9	0.86	50.5 ± 6.0	14.4 ± 0.8	8 ± 14	9.5 ± 1.0	14.2 ± 0.0	−0.6 ± 0.1	0 ± 0.1	4.2 ± 0.1	0.4	0.7
YZD-3	Cold	1.0 ± 1.1	4.8 ± 1.0	1.13	63.5 ± 14.0	15.1 ± 2.0	157 ± 253	16.2 ± 5.0	14.2 ± 0.1	−0.1 ± 0.2	−0.2 ± 0.4	4.5 ± 0.2	3.7	1.6
DF-1	Warm	3.6 ± 4.6	3.1 ± 1.0	2.19			134 ± 242	25.9 ± 2.3					0.5	1.5
DF-2	Warm	4.3 ± 4.6	3.7 ± 0.7	2.54			125 ± 201	25.0 ± 3.0					0.4	2.7
DF-3	Warm	3.3 ± 2.2	4.1 ± 0.9	2.25			118 ± 218	24.2 ± 2.5					0.4	2.6
DF-1	Cold	0.7 ± 1.2	6.9 ± 1.9	1.48	42.2 ± 10.5	12.6 ± 5.0	22 ± 41	8.9 ± 1.0	13.8 ± 0.0	−0.6 ± 0.1	−0.1 ± 0.1	3.5 ± 0.2	0.7	2.5
DF-3	Cold	0.9 ± 1.0	4.5 ± 1.2	1.60	60.8 ± 19.1	7.8 ± 2.7	26 ± 44	8.3 ± 1.2	13.5 ± 0.1	−0.6 ± 0.1	0 ± 0	1.8 ± 0.1	0.3	2.9
SFY-1	Warm	3.7 ± 4.5	15.1 ± 3.8	1.40			46 ± 93	21.8 ± 1.3						0.9
SFY-2	Warm	2.3 ± 3.1	5.6 ± 1.3	1.35			133 ± 187	24.2 ± 3.5						0.5
SFY-3	Warm	4.3 ± 5.3	6.7 ± 2.0	2.12			114 ± 164	23.5 ± 2.8						0.7
SFY-1	Cold	1.3 ± 2.2	6.0 ± 0.4	1.1			6 ± 12	5.8 ± 0.4					0.2	1.2
SFY-2	Cold	1.2 ± 2.7	8.8 ± 1.2	0.87			61 ± 108	9.7 ± 1.4					0.1	0.8
SFY-3	Cold	1.3 ± 2.4	9.4 ± 1.6	1.24			15 ± 33	9.2 ± 1.1					0.1	1.4

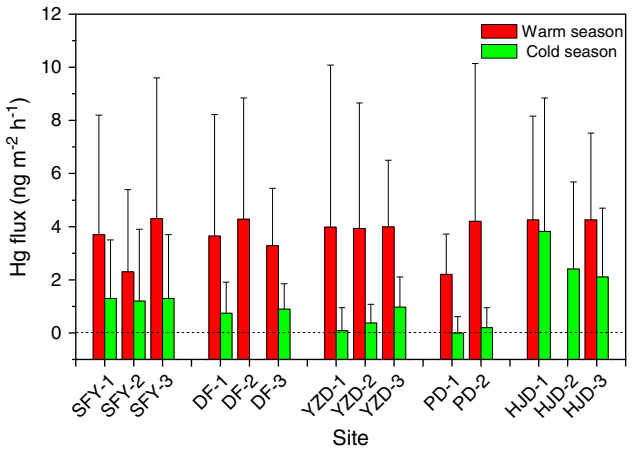

Figure 2. Spatial variations of Hg fluxes in warm and cold seasons.

parameters including water THg concentration, solar radiation, water TSS concentrations, and light penetration in water column in the HJD reservoir were relatively higher than other reservoirs, which are likely factors regulating RHg and DGM productions in the study area.

[16] No clear spatial variations in Hg flux were observed in the study area in warm season (Figure 2, t test, $p = 0.28$), and the mean fluxes of Hg from surface water ranged from 2.2 to 4.3 ng m^{-2} h^{-1}. On the other hand, water/air Hg fluxes differed significantly from different reservoirs in cold season (t test, $p < 0.05$). The Hg fluxes in HJD reservoir were about twofolds to threefolds higher than those measured in the other four reservoirs. Overall, the spatial variation of Hg fluxes is in good agreement with that of RHg and DGM concentrations (with the exception of PD-2 in warm season), indicating these Hg forms were important variables regulating water/air Hg flux in the study area. The elevated mean Hg flux at PD-2 in warm season accompanied by relatively lower mean RHg concentration may suggest some other factor, including other Hg forms in water, wind speed, and microbial activity, may also influence Hg fluxes in the study area (Table 2 and section 3.3).

[17] A clear and consistent seasonal variation with increased water/air Hg fluxes in warm season was observed throughout the study area (Table 2). As shown in Figure 2, average Hg fluxes in warm season were more than 2 times higher than those observed in cold season at all the sampling sites. In general, many studies found that the intensity of solar irradiation is an important factor influencing the diurnal cycle of water/air Hg flux, as a strong linearly positive correlation between Hg flux and solar radiation was observed [*Gårdfeldt et al*., 2001; *Feng et al*., 2004; *Zhang et al*., 2006a]. This is also the case at all the sampling sites in the present study (Figure 3). However, it is suggested that the seasonal variation of Hg flux was not mainly affected by the seasonal variation of solar radiation. For instance, the intensities of solar irritation at PD-1 and YZD-3 in cold season were significantly higher than the corresponding sites in warm season, which are in contrast to Hg fluxes (Table 2).

[18] Seasonal variations of RHg and DGM were investigated in HJD and PD reservoirs. RHg concentrations in both HJD and PD reservoirs exhibited a clear seasonal distribution pattern (t test, $p < 0.05$ for both). The mean RHg concentrations in PD and HJD reservoirs in warm season were about 1.9 and 1.5 times higher than those observed in cold season, respectively. No significant seasonal difference in DGM concentrations was observed for PD and HJD reservoirs (t test, $p > 0.05$ for both). The seasonal variation of RHg concentrations was probably caused by the seasonal cycles of weather and water chemistry conditions, as water THg and TSS concentrations, intensity of solar irritation, and air temperature experienced a similar seasonal pattern as RHg concentrations in surface water. A previous study by *Zhang et al*. [2006b] observed a clear monthly trend of DGM concentrations in surface water of the Can Creek Lake, and it was also suggested that it was mainly affected by monthly mean intensity of solar irradiation. The lack of seasonal trend in DGM concentrations in the study area may indicate some other factors and processes including THg and RHg concentrations, water light transmittance, and microbial activity in addition to sunlight-induced processes could also contribute to DGM variations.

3.2. Productions of RHg in Freshwaters and Potential Mechanisms

[19] Figures 4a and 4b show the diurnal variations of RHg and DGM in the study reservoirs, which may help to elucidate the potential mechanisms and factors contributing to RHg and DGM productions in the study area. The hourly RHg and DGM presented here were means of concentrations observed at sites (two to three sites) within each of the reservoir. RHg concentrations in surface waters of the study area exhibited a consistent diurnal trend with peak RHg concentrations at noon or in early afternoon and minimum concentrations at midnight or in early morning throughout the sampling campaigns. Significant correlations between RHg concentrations and intensity of solar irradiation were observed at all the sampling sites in the five reservoirs (t test, $p < 0.05$ for all). This suggests that sunlight-induced production was an important source of RHg in the study area. There are two possible pathways contributing to sunlight-induced production of RHg. It was suggested that sunlight may stimulate the activity of Hg^{2+} and accelerate the desorption process of Hg^{2+} from solid substrate in water [*Krabbenhoft et al*., 1998], which consequently drove an increase of RHg concentration under solar condition. Also, photodegradation of MeHg and photochemical oxidation of DGM might also contribute to the additional formation of RHg in waters [*Siciliano et al*., 2002; *Naftz et al*., 2011]. However, it should be noted that the DGM concentrations in the study areas were much lower than RHg concentrations, and the reported oxidation rate of DGM in fresh waters was much lower than photo-induced reduction of RHg [*Amyot et al*., 1997]. It is therefore speculated that the transformation of DGM to RHg might play a minimal role in RHg production in the study area. On the other hand, MeHg concentrations in study areas were reported to be in the range of 90–320 pg L^{-1} [*Zhang et al*., 2009; *Meng et al*., 2010; *Yao et al*., 2011], and previous study by *Naftz et al*. [2011] observed a more than 50% photodegradation of MeHg during day in the Great Salt Lake. It is therefore speculated that the photodegradation of MeHg during daytime might be an important mechanism contributing to the diurnal variations of RHg.

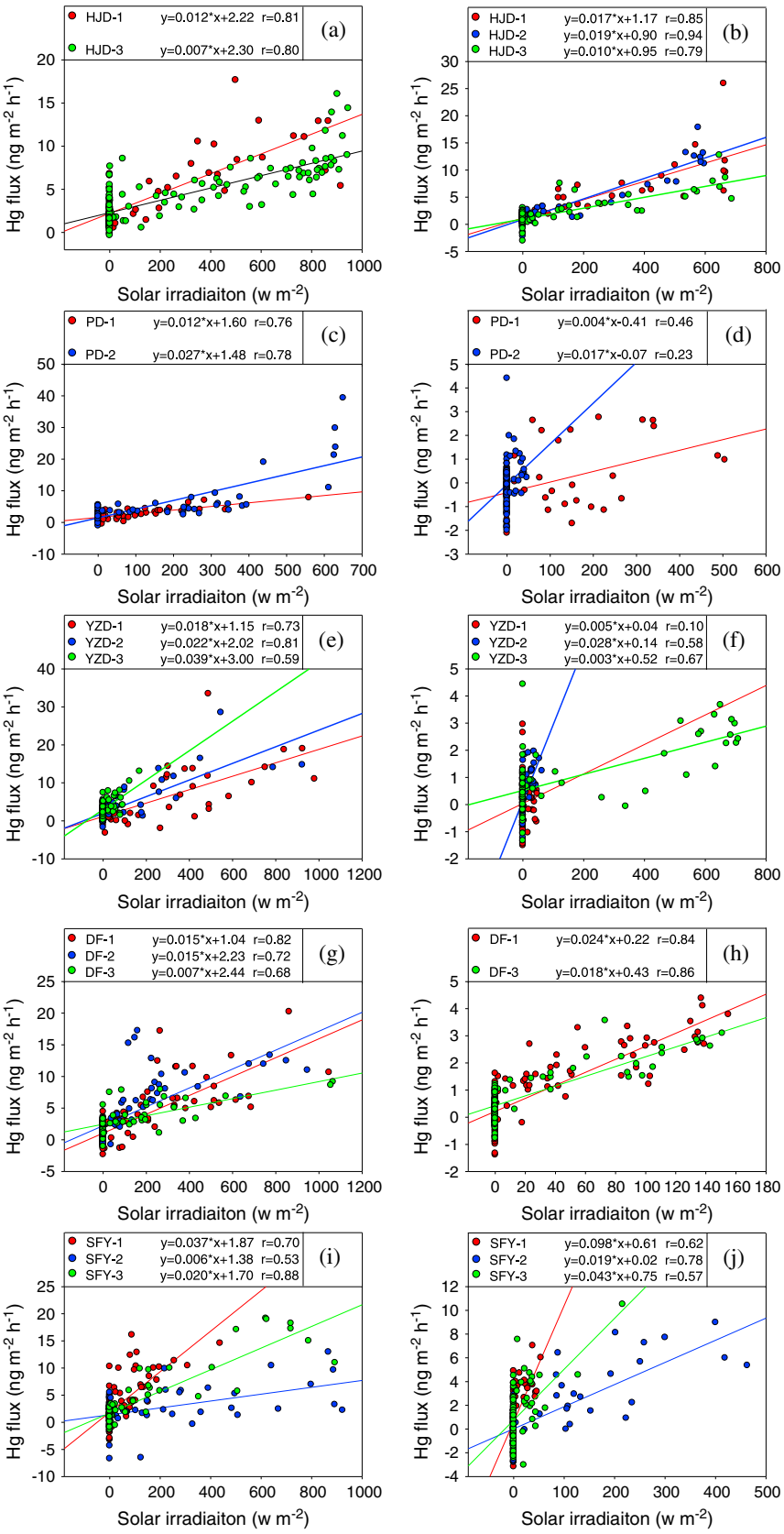

Figure 3. Linear correlations between solar irradiation and Hg flux in (a) HJD reservoir in warm season, (b) HJD reservoir in cold season, (c) PD reservoir in warm season, (d) PD reservoir in cold season, (e) YZD reservoir in warm season, (f) YZD reservoir in cold season, (g) DF reservoir in warm season, (h) DF reservoir in cold season, (i) SFY reservoir in warm season, and (j) SFY reservoir in cold season.

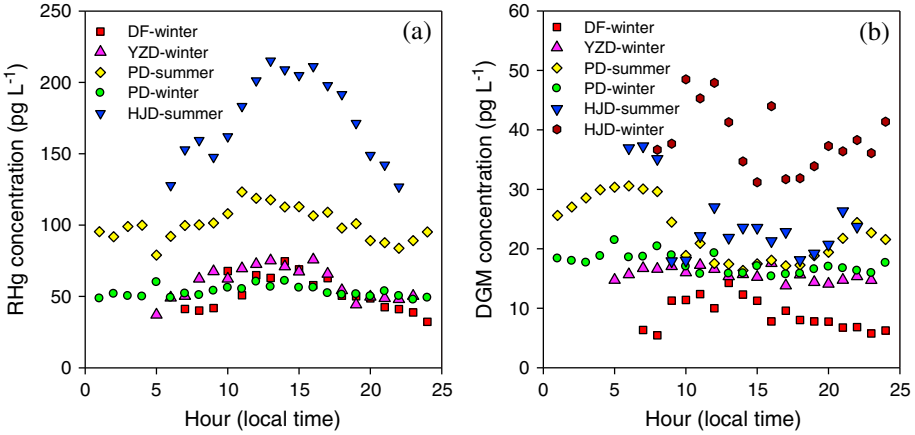

Figure 4. Diurnal trends in RHg and DGM concentrations at sites in the study area (plot indicates mean DGM concentration of the two to three sampling sites in each of the reservoir).

[20] The sunlight-induced production rates of RHg differed clearly from the studied reservoirs. The highest mean production rate of RHg (12.5 pg L^{-1} h^{-1}) was observed in HJD reservoir in warm season, followed by YZD in cold season (4.7 pg L^{-1} h^{-1}), DF in cold season (4.2 pg L^{-1} h^{-1}), PD in warm season (3.6 pg L^{-1} h^{-1}), and PD in cold season (1.3 pg L^{-1} h^{-1}). In order to gain a better insight to the factors regulating RHg distributions in the study area, correlations between means of RHg concentrations and water chemistry and weather parameters at different sites were investigated. As shown in Figure 5a, a significantly positive correlation was observed between surface water RHg concentrations and intensity of solar irritation, indicating sunlight-induced production might be an important processes contributing to RHg formations in the study area. Additionally, levels of RHg in the study area also tended to be affected by THg concentrations in surface water (Figure 5b). However, the strong correlation between RHg and THg concentration does not clarify that THg in water could be a substrate for photo-induced RHg production. Actually, some previous studies in Wujiang River basin revealed that many mercury forms including dissolved mercury, particulate-bounded mercury, and methyl mercury had strong positive correlations with THg concentrations [*Guo*, 2008b; *Zhang et al*., 2009], and it is still unclear which form of water Hg constituted to be the major substrate of RHg production. A negative correlation between RHg concentrations and TSS contents in surface water was also observed in the study area (Figure 5c). The correlation was not significant at $p < 0.05$ level because TSS was not the major variable influencing RHg in the study area. However, the negative relationship may suggest that lower content of TSS in water tended to facilitate the production of RHg by limiting the sorption processes and increasing the depth of light transmittance layer.

[21] Using a stepwise linear Pearson correlation analysis, we developed an empirical model with three key variables of THg concentration, solar irradiation, and TSS concentration to predict the spatial distributions of RHg in the study area (equation 7) as follows:

$$\mathrm{RHg} = 0.0625 \times [\mathrm{THg}] + 0.022 \times [\text{solar irradiation}] - 23.5 \times [\mathrm{TSS}] + 12.4 \quad (7)$$

[22] The three variables showed significant correlations with RHg concentrations in the modeling equation at $p < 0.05$ level. A good agreement (paired t test, $p = 0.955$) between measured and predicted RHg concentrations was obtained using equation (7).

3.3. Productions of DGM in Freshwaters and Potential Mechanisms

[23] DGM concentrations experienced different diurnal cycles in different reservoirs. In DF reservoir, DGM

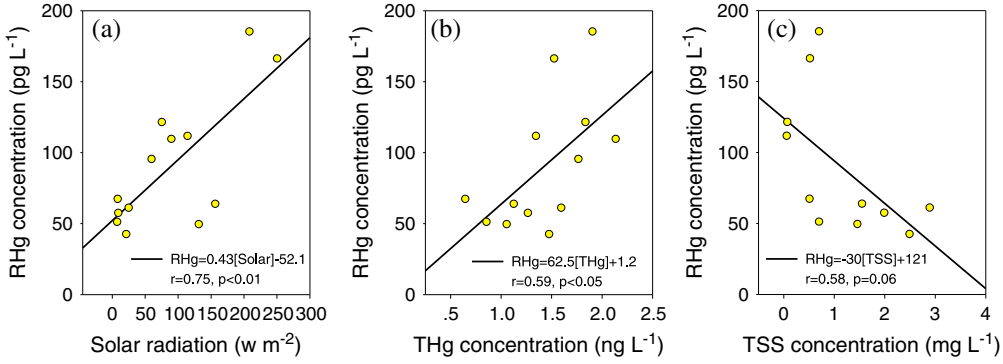

Figure 5. Correlations between RHg concentrations and solar radiation, THg concentrations, and TSS contents.

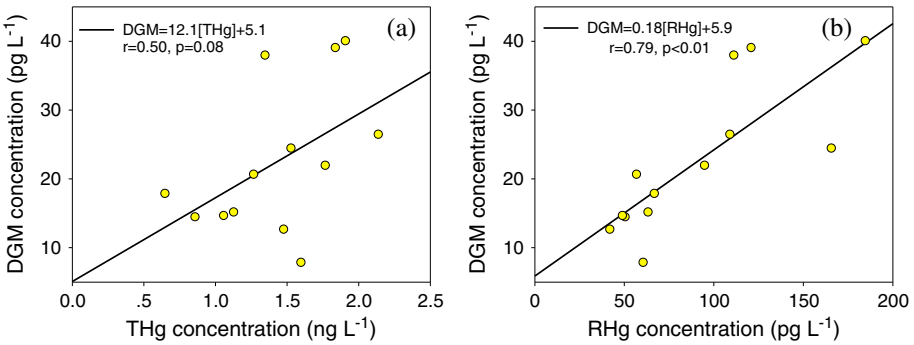

Figure 6. Correlations between DGM concentrations and THg and RHg concentrations.

exhibited a clear diurnal variation with elevated concentrations during daytime and decreased concentrations at night (Figure 4b). The diurnal DGM pattern in DF reservoir is quite similar to that reported by many previous literatures [*O'Driscoll et al*., 2003; *Zhang et al*., 2006a]. Significantly positive correlations were observed between DGM concentrations and intensity of solar irradiation ($r_{DF\text{-}1} = 0.66$, $r_{DF\text{-}2} = 0.74$, $p < 0.01$ for both) and RHg concentrations ($r_{DF\text{-}1} = 0.5$, $p < 0.05$; $r_{DF\text{-}1} = 0.89$, p 0.01) at two sites in DF reservoir, suggesting that sunlight-induced reductions of RHg might play an important role in the production of DGM in DF reservoir.

[24] DGM concentrations showed a distinct diurnal cycle in PD reservoir (Figure 4b). DGM concentrations in PD reservoir increased continuously after sunset and peaked at midnight and early morning, then decreased throughout the day. This diurnal pattern was more pronounced in warm season compared to cold season (Figure 4b). The diurnal cycle of DGM concentration in PD reservoir is in contrast to many of the previous studies which suggested that sunlight-induced processes played a major role in DGM distributions in waters [*Gårdfeldt et al*., 2001; *O'Driscoll et al*., 2003; *Zhang et al*., 2006b]. It is speculated that increased DGM concentrations at night were attributed to bacteria-induced production built upon decreased sunlight-mediated oxidation and evaporation of DGM. It has been reported that heterotrophic bacteria played a dominant role in DGM production in freshwater of Sweden even under dark conditions [*Mason et al*., 1995]. PD reservoir is a eutrophic reservoir with a mean bacteria abundance up to 3 times higher than the means in other reservoirs in the study areas [*Wang et al*., 2008], and this is likely attributable to the enhanced bacteria-induced production of DGM in this reservoir.

[25] The peak concentrations of DGM in HJD and YZD were observed before noon, then decreased significantly, and showed the lowest values in the afternoon. This trend suggests production and loss of DGM were occurring simultaneously during daytime. The peak concentrations before noon most likely resulted from sunlight-induced production of DGM; whereas photo-induced oxidation and evaporation of DGM from water became dominant in the afternoon, which constituted to be the major reason for decreased DGM concentrations in the afternoon.

[26] No significant correlation was observed between mean DGM and THg concentrations in the study area (Figure 6a), which is different from RHg. The mean levels of DGM at different sites were significantly correlated with mean RHg concentrations (Figure 6b). Since the RHg concentration in the study areas were much higher than DGM concentrations and the reported oxidation rate of DGM in freshwaters was much lower than photo-induced reduction of RHg [*Amyot et al*., 1997], it is speculated that RHg in water was a major substrate for DGM production and regulated the distribution of DGM in the study area. Additionally, a significantly negative correlation was also observed between mean DGM concentrations and TSS content in waters of the sampling sites ($r = 0.74$, $p < 0.01$, figure not shown). This implies that lower TSS contents may favor DGM production in waters by increasing the lability of reducible Hg^{2+} complexes and light transmittance in water column (Table 2, lower TSS contents correspond to higher light transmittance).

3.4. Probing the Major Factors Controlling Water/Air Hg Flux From Freshwaters

[27] Exchange flux of Hg between water and air interface is a dynamic process affected by a combination of many water chemical and meteorological parameters. The effects of meteorological parameters including solar irradiation, water and air temperature, and wind speed on the diurnal cycle of Hg fluxes have been well studied by many previous studies [*Poissant and Casimir*, 1998; *Zhang et al*., 2006a; *Feng et al*., 2008]. However, the correlations between Hg fluxes and concentrations of mercury species in different water environments were not well investigated, which are crucial for better estimates of mercury emission from natural waters from a local to a global scale.

[28] Figure 7 shows the overall correlations between mean Hg fluxes and THg, RHg, and DGM concentrations at all the sites in the study area. Significantly positive correlations were observed between Hg fluxes and THg, RHg, and DGM concentrations, indicating variations of Hg flux from waters were probably related to the distribution and production of THg, RHg, and DGM in the study area. For the three forms of Hg in surface waters, the most pronounced correlation was observed between Hg fluxes and RHg concentrations (Figure 7). This may suggest that level of RHg in surface water was a crucial variable affecting Hg evasion flux in the study area. Alternatively, however, the strong correlation between RHg concentrations and Hg fluxes may also partially result from the fact that both RHg concentrations and Hg fluxes were related to sunlight-mediated processes of THg (the fraction of THg without RHg). A previous study by *Amyot et al*. [1997] reported that about 2–7% of the RHg in freshwaters could

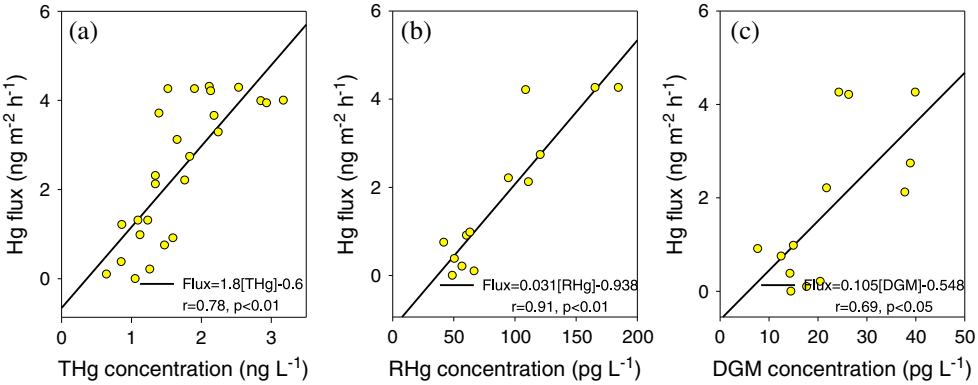

Figure 7. Correlations between Hg fluxes and THg, RHg, and DGM concentrations.

be reduced to DGM in 1 h under cloudy and sunny weather conditions. Assuming that 4% of the RHg in the light transmittance layer of upper water column (lower limit: 1 m) is available for DGM production and Hg flux to the atmosphere in 1 h, the mean fluxes are roughly estimated to be 1.6–7.2 ng m^{-2} h^{-1}, which are much higher than the measured mean fluxes in the study area (Table 2). This assumption suggests that the strong correlation between RHg concentrations and Hg fluxes may not be a major reflection of sunlight-mediated processes of THg, and reduction of RHg in the upper layer of waters could be an important mechanism contributing to Hg flux.

[29] A significantly positive correlation between DGM concentrations and Hg fluxes was also observed in the study area. This is consistent with the thin film gas exchange model which demonstrates that Hg flux from water is mainly driven by the diffusion of DGM from water to the atmosphere [*Xu et al*., 1999; *Poissant et al*., 2000]. However, the simulated Hg fluxes were much lower than measured fluxes in the study area (Table 2). The significant difference may suggest the DFC method overestimated water/air Hg flux, probably due to the relatively higher flushing flow rate (8–15 L min^{-1}) employed in the present study which has not been evaluated for water/air flux by previous studies. Alternatively, results simulated by the thin film model were significantly underestimated. The gas transfer velocity of Hg^0 (K_w), which is an important variable regulating simulation of Hg flux from waters, is mainly dominated by wind speed. The wind speeds in the study area were quite low (0.1–3.7 m s^{-1} with median of 0.6 m s^{-1}) during the study period. The k_w was not well characterized for low wind speed conditions and might be underestimated in the presented study [*Poissant et al*., 2000; *O'Driscoll et al*., 2003]. Another possible criticism related to the thin film model is not capable to depict the role of depth profile of DGM concentration and diffusion in surface water on water/air Hg flux. The surface waters in PD, YZD, and DF reservoirs were consistently unsaturated in terms of DGM due to low DGM concentrations in water and elevated TGM concentrations in ambient air (Table 2). This is in contrast with positive Hg fluxes (means: 0.4 ~ 1.5 ng m^{-2} h^{-1} during DGM sampling periods) measured by DFC method. Due to direct exposure of sunlight and photoreductions of previous deposited atmospheric reactive mercury, water/air interface may be enriched with DGM compared to sublayers under the interface especially under low wind speed conditions. The water samples in the present study were collected at a depth of 2–4 cm below the water surface, which likely underestimated DGM concentrations at the water/air interface and in turn yielded relatively lower predicted fluxes. It is also unclear whether the evaporation of Hg^0 at the water/air interface is controlled by the transfer velocity of Hg^0 (K_w) or the calculations of K_w should be modified for Hg^0 diffusion at the water/air interface. Hence, further investigations on the estimate of K_w for freshwaters under low wind speed condition and DGM dynamics in the surface waters are needed.

[30] It is also observed that Hg fluxes were significantly correlated with air temperature ($r = 0.84$, $p < 0.01$). It may be partially attributed to the fact that air temperature was significantly correlated with solar irradiation ($r = 0.74$, $p < 0.01$) which has been proved to be an important variable regulating Hg flux from water [*Boudala et al*., 2000; *Feng et al*., 2004]. However, it should be pointed out that the correlation between air temperature and Hg fluxes was more pronounced compared to solar irradiation ($r = 0.57$, $p < 0.01$), suggesting that other processes related to air temperature may also affect Hg flux in the study area. It was reported that increased water temperature tended to promote microbial activities [*Mason et al*., 1995]. Water temperatures were not measured at all the sampling sites, but air temperature was significantly linearly correlated with water temperature in the study area ($r = 0.92$, p 0.01), which may partially explain the strong correlation between air temperature and Hg fluxes. Additionally, according to the thin film gas exchange model [*Poissant et al*., 2000; *Gårdfeldt et al*., 2003b; *O'Driscoll et al*., 2003], temperature is also an important variable influencing diffusion process of DGM from water to the atmosphere by means of regulating the Henry's law constant of Hg^0 between water and atmosphere [*Andersson et al*., 2008]. Although these results do not imply that air temperature played a more important role in influencing Hg flux compared to solar irradiation, we speculate that air temperature may be a better precursor for predicting Hg fluxes from water in our study area.

3.5. Model Development of Hg Flux From Freshwaters and Estimates of Hg Emissions From Reservoirs in Wujiang River

[31] Modeling studies on predicting water/air exchange flux have been conducted in many previous literatures. A

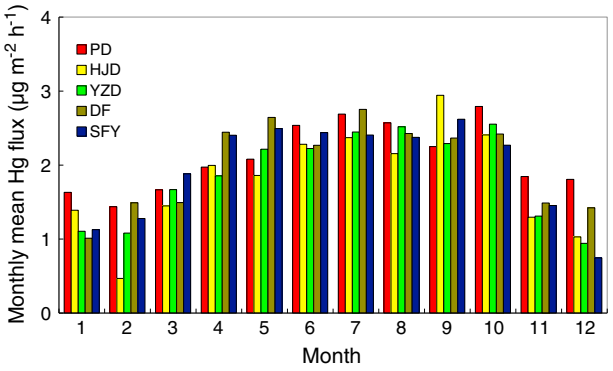

Figure 8. Monthly variations of simulated water/air Hg fluxes in the study area.

thin film gas exchange model developed by *Wanninkhof* [1992] has been modified for mercury and widely employed in both freshwaters [*Poissant et al*., 2000; *O'Driscoll et al*., 2003] and seawaters [*Wängberg et al*., 2001; *Gårdfeldt et al*., 2003b; *Fu et al*., 2010b]. As shown in section 3.4, however, the thin film gas exchange model significantly underestimated water/air Hg fluxes in the study area. *Zhang et al*. [2006a] evaluated the sensitivity of different models in predicting water/air Hg flux in the Bay Saint François wetlands. They proposed that a thin film model modified by net solar irradiation and a specific model with only one variable of solar irradiation could better simulate Hg flux from water. In the study area, it was observed that DGM concentrations and intensity of solar irradiation were less significant variables in controlling Hg fluxes, compared to THg and RHg concentrations and air temperatures. Moreover, surface waters in the study area were in general unsaturated in term of DGM in cold season (Table 2), and this indicates that simplified model with one variable of solar irradiation is not valid in the study area [*Zhang et al*., 2006a].

[32] As mentioned in section 3.1, water Hg fluxes exhibited clear spatial and temporal variations in the study area. This is likely attributable to variations of water chemical parameters and meteorological factors, which should be taken into account when developing models. Since RHg and DGM in water are much active and tends to be subjected to loss, reproduction, and contamination during storage time, it is very difficult to be precisely measured without in situ experiments. Therefore, RHg and DGM were not selected for developing water/air Hg flux model. THg concentration, TSS content, air TGM concentration, and metrological parameters were classified into two major components using the Statistical Production and Service Solution (SPSS) factor analysis method. One component includes THg concentration, TSS content, and humidity, whereas the other component includes solar irradiation, air temperature, and air TGM concentration. On the basis of a stepwise linear Pearson correlation analysis, THg concentration and air temperature were selected to represent the two major components which could better simulate Hg flux in the study area. The established model was shown as below:

$$F = 1.02 \times [\mathrm{THg}] + 0.12 \times [\mathrm{Temp_{Air}}] - 1.29 \qquad (8)$$

where F is the Hg flux from water (ng m^{-2} h^{-1}), THg is the THg concentration in surface water (ng L^{-1}), and $Temp_{Air}$ is the air temperature (°C). The simulated Hg fluxes using equation (8) showed a good agreement with measured values in the study area (paired *t* test, $p = 0.96$).

[33] To estimate the annual Hg emissions from the studied reservoirs, monthly THg concentrations in surface waters [*Guo*, 2008b] and monthly mean air temperature of the five reservoirs were employed as inputs in the developed model. The calculated monthly mean Hg fluxes in the study area are shown in Figure 8. All the reservoirs in the study area were net sources of Hg to the atmosphere, with monthly mean Hg fluxes ranging from 0.5 to 2.9 μg m^{-2} mon^{-1}. The maximum annual mean flux was observed in PD reservoir, which corresponds well to the elevated THg concentrations in the reservoir. Hg fluxes showed a clear seasonal pattern at all the reservoirs in the study area, with elevated emission fluxes observed in warm season, which is mainly related to monthly variations of air temperature. The water/air emission fluxes of Hg in the study area are relatively lower than the bulk precipitation fluxes of Hg (Table 1), indicating reservoirs in the study area are net sinks of atmospheric Hg. Given the total surface areas of the reservoirs (Table 1), the annual water Hg emission in the study area was estimated to be 3.2 ± 1.0 kg.

3.6. Implication of Mercury Dynamics in Reservoirs

[34] Mercury dynamics in aquatic environments is of particular concern due to the production of neurotoxic MeHg which can be bioaccumulated and biomagnified in the food chain. Some previous studies have revealed that the constructions of reservoir could facilitate the microbial methylation of inorganic mercury to MeHg owing to the decomposition of organic carbon in submerged soil [*Hall et al*., 2004; *Feng et al*., 2009a, 2009b]. One of the major ecological criticisms for development of reservoirs is the hydrological alteration of the aquatic environments. Water flow rate can be significantly decreased after the construction of reservoir, which in turn decreases the content of suspended solid substrates in the upper layer of water column and minimizes the vertical mixing of chemical, physical, or biological parameters. As discussed earlier, decreased suspended solid substrates tend to facilitate the productions of RHg and DGM in the light transmittance water layer, and this likely drives an increase in Hg evasion and a decrease of concentrations of MeHg in the upper water layer of reservoirs. Moreover, the vertical transport of RHg from surface water to the deeper portion of water column and sediment, which is an important substrate of Hg methylation, will be limited due to the thermal stratification formed in the water column. It was reported that the mean MeHg concentrations in water column of HJD reservoir were relatively lower than those observed from other reservoirs in the study area [*Zhang et al*., 2009; *Meng et al*., 2010; *Yao et al*., 2011], whereas DGM and RHg concentration in surface water of HJD were relatively elevated (Table 2). This may be partially attributable to the lower water flow rate and TSS contents in HJD reservoir (Table 1).

[35] However, it does not clarify that these mechanisms dominated the fate of MeHg in the study area, and the dynamic of mercury species in water column is still unclear. For instance, it is unknown whether the decreasing vertical mixing will result in an overall lower photodegradation in

the water column or not. Also, anoxic condition in the deep water built upon the thermal stratification of the water column may also favor Hg methylation at deep water and sediment, which consequently increases the levels of MeHg in the water column by diffusion processes. For the reservoirs in the study area, it is possible that adjustments of water hydrological conditions using periodically hydroelectric power generation may favor the production of MeHg and limit degradation of MeHg. Thus, investigations with respect to depth profiles for mercury species including RHg, DGM, and MeHg related to the adjustment of hydrological conditions in the reservoirs should be addressed in future studies.

4. Summary and Conclusions

[36] A study was carried out to investigate the seasonal, diurnal, and spatial variations of water/air exchange fluxes of Hg, RHg, and DGM concentrations in surface waters at 14 sites in five reservoirs, Wujiang River Basin, Southwest China. The means of Hg fluxes, RHg, and DGM concentrations in the study areas were in the ranges of 0–4.3 ng m^{-2} h^{-1}, 42.2–184.9 pg L^{-1}, and 7.8–40.0 pg L^{-1}, respectively, which are slightly lower than those observed in wetlands and anthropogenic impacted watersheds.

[37] RHg concentrations showed a consistent diurnal trend with increasing concentrations during day at all the sampling sites. The diurnal trend of RHg concentrations was strongly related to incident intensity of solar irradiation, indicating production of RHg in the study area was mainly stimulated by sunlight. Mean RHg concentrations differed significantly at different sites, and the levels of THg and TSS in water played an important role in the spatial patterns of RHg.

[38] No consistent diurnal pattern in DGM concentrations was observed. The diurnal cycle with elevated DGM concentrations at night in PD reservoir, which was a eutrophic reservoir with relatively higher bacteria abundance, was probably related with bacteria-induced processes. For other reservoirs, sunlight-induced production of DGM was responsible to the peaks observed before or at noon, and then sunlight-induced oxidation and evaporation of Hg^0 became dominant and resulted in the decreasing trend of DGM in the afternoon. Mean DGM concentration at each site was significantly positively correlated with mean RHg concentration and negatively correlated with TSS concentration. This may suggest RHg in surface water was a major substrate for DGM production. Lower TSS concentration in water was thought to increase the liability of Hg(II) and light transmittance depth in water column, which may favor DGM production in the study area.

[39] The overall spatial distribution of Hg fluxes was most significantly correlated with RHg concentrations, followed by THg and DGM concentrations. Spatial variation of Hg fluxes exhibited a more pronounced correlation with air temperature compared to solar irradiation. It is hypothesized that air temperature may be a better precursor for predicting Hg fluxes from water. THg concentration and air temperature were selected in developing an empirical model, and this model could well simulate the variation of Hg fluxes in the study area. Total annual emission of Hg from the study area was estimated to be 3.2 ± 1.0 kg.

[40] **Acknowledgments.** This research was financially supported by the National Basic Research Program of China (973 program-2013CB430003), with additional support from the Innovative Program (Special Foundation for Young Scientist) of The Chinese Academy of Sciences (KZCX2-EW-QN111), and National Science Foundation of China (41003051, 41273145, 41030752).

References

Amyot, M., G. Mierle, D. Lean, and D. J. McQueen (1997), Effect of solar radiation on the formation of dissolved gaseous mercury in temperate lakes, *Geochim. Cosmochim. Acta*, *61*, 975–987.

Amyot, M., F. M.M. Morel, and P. A. Ariya (2005), Dark oxidation of dissolved and liquid elemental mercury in aquatic environment, *Environ. Sci. Technol.*, *39*, 110–114.

Andersson, M. E., K. Gårdfeldt, I. Wängberg, and D. Strömberg (2008), Determination of Henry's law constant for elemental mercury, *Chemosphere*, *28*, 587–592.

Boudala, F. S., I. Folkins, S. Beauchamp, R. Tordon, J. Neima, and B. Johnson (2000), Mercury flux measurements over air and water in Kejimkujik National Park, Nova Scotia, *Water Air Soil Pollut.*, *122*, 183–202.

Cosovic, B., I. Ciglenecki, D. Vilicic, and M. Ahel (2000), Distribution and seasonal variability of organic matter in a small eutrophied salt lake, *Estuar. Coast. Shelf.*, *S51*, 705–715.

Costa, M., and P. Liss (2000), Photoreduction and evolution of mercury from seawater, *Sci. Total Environ.*, *261*, 125–135.

Eckley, C. S., M. S. Gustin, C. -J. Lin, X. Li, and M. B. Miller (2010), The influence of dynamic chamber design and operating parameters on calculated surface-to-air mercury fluxes, *Atmos. Environ.*, *44*, 194–203.

Feng, X., H. Yan, S. Wang, G. Qiu, S. Tang, L. Shang, Q. Dai, and Y. Hou (2004), Seasonal variation of gaseous exchange between air and water surface over Baihua reservoir, Guizhou, China, *Atmos. Environ.*, *38*, 4721–4732.

Feng, X., S. Wang, G. L. Qiu, H. T. He, G. H. Li, and Z. G. Li (2008), Total gaseous mercury exchange between water and air during cloudy weather conditions over Hongfeng Reservoir, Guizhou, China, *J. Geophys. Res.*, *113*, D15309. doi:10.1029/2007JD009600.

Feng, X., H. Jiang, G. Qiu, H. Yan, G. Li, and Z. Li (2009a), Geochemical processes of mercury in Wu-Jiang-Du and Dong-Feng reservoirs, Guizhou, China, *Environ. Pollut.*, *157*, 2970–2984.

Feng, X., H. Jiang, G. Qiu, H. Yan, G. Li, and Z. Li (2009b), Mercury mass balance study in Wu-Jiang-Du and Dong-Feng reservoirs, Guizhou, China, *Environ. Pollut.*, *157*, 2594–2603.

Fu, X. W., X. B. Feng, Q. Wan, B. Meng, H. Y. Yan, and Y. N. Guo (2010a), Probing Hg evasion from surface waters of two Chinese hyper/meso-eutrophic reservoirs, *Sci. Total Environ.*, *408*, 5887–5896.

Fu, X. W., et al. (2010b), Mercury in the marine boundary layer and seawater of the South China Sea: Concentrations, sea/air flux, and implication for land outflow, *J. Geophys. Res.*, *115*, D06303. doi:10.1029/2009JD012958.

Garcia, E., J. Laroulandie, X. R. Saint-Simon, and M. Amyot (2006), Temporal and spatial distribution and production of dissolved gaseous mercury in the Bay St. François wetland, in the St. Lawrence River, Quebec, Canada, *Geochim. Cosmochim. Acta*, *70*, 2665–2678.

Gårdfeldt, K., X. B. Feng, J. Sommar, and O. Lindqvist (2001), Total gaseous mercury exchange between air and water over lake and sea surfaces, *Atmos. Environ.*, *35*, 3027–3038.

Gårdfeldt, K., M. Horvat, J. Sommar, J. Kotnik, V. Fajon, I. Wängberg, and O. Lindqvist (2002), Comparison of methods for measurements of dissolved gaseous mercury in seawater performed on a Mediterranean cruise, *Anal. Bioanal. Chem.*, *28*, 1002–1008.

Gårdfeldt, K., J. Munthe, D. Störmberg, and O. Lindqvist (2003a), A kinetic study on the abiotic methylation of divalent mercury in the aqueous phase, *Sci. Total Environ.*, *304*, 127–136.

Gårdfeldt, K., et al. (2003b), Evasion of mercury from coastal and open waters of the Atlantic Ocean and Mediterranean Sea, *Atmos. Environ.*, *37*, 73–84.

Guo, Y. N. (2008b), Input and output fluxes of mercury in different evolutive reservoirs in Wujiang River Basin, PH.D. dissertation, Graduate University of the Chinese Academy of Science, Bejing, China (in Chinese with abstract in English).

Guo, Y. N., X. B. Feng, Z. G. Li, T. R. He, H. Y. Yan, and B. Meng (2008a), Distribution and wet deposition fluxes of total and methyl mercury in Wujiang reservoir Basin, Guizhou, China, *Atmos. Environ.*, *42*, 7096–7103.

Hall, B. D., V. L. St. Louis, and R. A. Bodaly (2004), The stimulation of methylmercury production by decomposition of flooded birch leaves and jack pine needles, *Biogeochemistry*, *68*, 107–129.

Krabbenhoft, D. P., J. P. Hurley, M. L. Olson, and L. B. Cleckner (1998), Diel variability of mercury phase and species distributions in the Florida Everglades, *Biogeochemistry*, *40*, 311–325.

Kuss, J., J. Holzmann, and A. R. Ludwig (2009), Coefficient for natural waters determined by molecular dynamics simulation, *Environ. Sci. Technol.*, *28*, 3183–3186.

Lalonde, J. D., M. Aymot, J. Orvoine, F. M. M. Morel, J. -C. Auclair, and P. A. Ariya (2004), Photoinduced oxidation of Hg^0(aq) in the waters from the St. Lawrence Estuary, *Environ. Sci. Technol.*, *38*, 508–514.

Marvin-DiPasquale, M., and M. H. Cox (2007), Legacy mercury in Alviso Slough, South San Francisco Bay, California: Concentration, speciation and mobility: Menlo Park, CA, U.S. Geological Survey, Open-File Report number 2007–1240, 98p.

Mason, R. P., F. M. M. Morel, and H. F. Hemond (1995), The role of microorganisms in elemental mercury formation in natural waters, *Water. Air. Soil. Poll.*, *80*, 775–787.

Meng, B., X. B. Feng, X. X. Chen, G. L. Qiu, J. Sommar, and Y. N. Guo (2010), Influence of eutrophication on the distribution of total mercury and methylmercury in hydroelectric reservoirs, *J. Environ. Qual.*, *39*, 1–12.

Naftz, D. L., J. R. Cederberg, D. P. Krabbenhoft, K. R. Beisner, J. Whitehead, and J. Gardberg (2011), Diurnal trends in methylmercury concentration in a wetland adjacent to Great Salt Lake, Utah, USA, *Chem. Geol.*, *283*, 78–86.

O'Driscoll, N. J., S. Seauchamp, S. D. Siciliano, A. N. Rencz, and D. R. S. Lean (2003), Continuous analysis of dissolved gaseous mercury (DGM) and mercury flux in two freshwater lakes in Kejimkujik Park, Nova Scotia: Evaluating mercury flux models with quantitative data, *Environ. Sci. Technol.*, *37*, 2226–2235.

O'Driscoll, N. J., L. Poissant, J. Canário, and R. S. Lean (2008), Dissolved gaseous mercury concentrations and mercury volatilization in a frozen freshwater Fluvial Lake, *Environ. Sci. Technol.*, *42*, 5125–5130.

Peters, S. C., J. L. Wollenberg, D. P. Morris, and J. A. Porter (2007), Mercury emission to the atmosphere from experimental manipulation of DOC and UVR in mesoscale field chambers in a freshwater lake, *Environ. Sci. Technol.*, *41*, 7356–7362.

Poissant, L., and A. Casimir (1998), Water-air and soil-air exchange rate of total gaseous mercury measured at background sites, *Atmos. Environ.*, *32*, 883–893.

Poissant, L., M. Amyot, M. Pilote, and D. Lean (2000), Mercury water-air exchange over the upper St. Lawrence River and Lake Ontario, *Environ. Sci. Technol.*, *34*, 3069–3078.

Poulain, A. J., M. Amyot, D. Findlay, S. Telor, T. Barkay, and H. Hintelmann (2004), Biological and photochemical production of dissolved gaseous mercury in a boreal lake, *Limnol. Oceanogr.*, *49*, 2265–2275.

Qureshi, A., N. J. O'Driscoll, M. Macloed, Y. -M. Neuhold, and K. Hungerbühler (2010), Photoreactions of mercury in surface ocean water: Gross reaction kinetics and possible pathways, *Environ. Sci. Technol.*, *44*, 644–649.

Rolfhus, K. R., and W. F. Fitzgerald (2001), The evasion and spatial/temporal distribution of mercury species in Long Island Sound, CT-NY, *Geochim. Cosmochim. Acta*, *65*, 407–418.

Siciliano, S. D., N. J. O'Driscoll, and D. R. S. Lean (2002), Microbial reduction and oxidation of mercury in freshwater lakes, *Environ. Sci. Technol.*, *36*, 3064–3068.

Skyllberg, U., M. B. Westin, M. Meili, and E. Björn (2009), Elevated concentrations of methyl mercury in streams after Forest Clear-Cut: A consequence of mobilization from soil or new methylation? *Environ. Sci. Technol.*, *43*, 8535–8541.

Wang, B. L., C. Q. Liu, F. S. Wang, Y. X. Yu, and L. H. Zhang (2008), The distributions of autumn picoplankton in relation to environmental factors in the reservoirs along the Wujiang River in Guizhou Province, SW China, *Hydrobiologia*, *589*, 35–45.

Wängberg, I., S. Schmolke, P. Schager, J. Munthe, R. Ebinghaus, and Å. Iverfeldt (2001), Estimates of air-sea exchange of mercury in the Baltic Sea, *Atmos. Environ.*, *35*, 5477–5484.

Wanninkhof, R. (1992), Relationship between wind speed and gas exchange over the ocean, *J. Geophys. Res.*, *97*(C5), 7373–7382.

Xiao, Z, D. Strömberg, and O. Lindqvist (1995), Influence of humic substances on photolysis of divalent mercury in aqueous solution, *Water Air Soil Pollut.*, *80*, 789–798.

Xu, X. H., X. S. Yang, D. R. Miller, and J. J. Helble (1999), Formulation of bi-directional atmosphere-surface exchanges of elemental mercury, *Atmos. Environ.*, *33*, 4345–4355.

Yao, H., X. B. Feng, Y. N. Guo, H. Y. Yan, X. W. Fu, Z. G. Li, and B. Meng (2011), Mercury and methylmercury concentrations in two newly constructed reservoirs in the Wujiang River, Guizhou, China, *Toxicol., Chem.*, *30*, 530–537.

Zhang, H., and S. E. Lindberg (2001), Sunlight and iron(III)-induced photochemical production of dissolved gaseous mercury in freshwater, *Environ. Sci. Technol.*, *35*, 928–935.

Zhang, H., L. Poissant, X. H. Xu, M. Pilote, C. Beauvais, M. Amyot, E. Garcia, and J. Laroulandie (2006a), Air−water gas exchange of mercury in the Bay Saint Francois wetlands: Observation and model parameterization, *J. Geophys. Res.*, *111*, D17307, doi:10.1029/2005JD006930.

Zhang, H., C. Dill, T. Kuiken, M. Ensor, and W. C. Crocker (2006b), Change of dissolved gaseous mercury concentrations in a southern reservoir lake (Tennessee) following seasonal variation of solar radiation, *Environ. Sci. Technol.*, *40*, 2114–2119.

Zhang, J. F., X. B. Feng, H. Y. Yan, Y. N. Guo, H. Yao, B. Meng, and K. Liu (2009), Seasonal distributions of mercury species and their relationship to some physicochemical factors in Puding Reservoir, Guizhou, China, *Sci. Total Environ.*, *408*, 122–129.